INTERNATIONAL TABLES FOR CRYSTALLOGRAPHY

ISSN 1574-8707
it.iucr.org

Volume I, X-ray Absorption Spectroscopy and Related Techniques
ISBN: 978-1-119-43394-1

Chapter 2.24

Keywords: nuclear resonance; Mössbauer effect; synchrotron radiation; inelastic scattering; sum rules.

Sum rules for the analysis of nuclear resonant absorption spectra

Ralf Röhlsberger[a,b,c]* and Michael Y. Hu[d]

[a]Deutsches Elektronen-Synchrotron DESY, 22607 Hamburg, Germany, [b]Helmholtz-Institut Jena, 07743 Jena, Germany, [c]Friedrich-Schiller Universität Jena, 07743 Jena, Germany, and [d]Advanced Photon Source, Argonne National Laboratory, Argonne, IL 60439, USA. *Correspondence e-mail: ralf.roehlsberger@desy.de

Nuclear resonant scattering of synchrotron radiation (NRS) has become an established tool in condensed-matter research. Synchrotron radiation, with its outstanding brilliance, transverse coherence and polarization, has opened this field to many unique studies. These range from fundamental research in the field of light–matter interaction to condensed matter physics and materials science. This applies in particular to the electronic and magnetic structure of very small sample volumes such as microstructures and nanostructures, and samples under extreme conditions of temperature and pressure. The application of high-resolution monochromatization techniques routinely allows one to record lattice dynamical properties via inelastic nuclear resonance excitation with sub-meV energy resolution. After a brief introduction to the NRS technique, this contribution provides an overview of how sum rules can be applied to NRS absorption spectra to reveal dynamical properties of condensed-matter systems.

1. Introduction

The extremely narrow nuclear resonances of Mössbauer nuclei are very sensitive probes of condensed-matter properties. A very prominent method in this field is Mössbauer spectroscopy, a technique that probes internal magnetic and electric fields in the sample by analysing the hyperfine splitting of the nuclear energy levels using the absorption of γ radiation. Customarily, this technique is applied in the energy domain, where the radiation from a monochromatic radioactive source is Doppler tuned to measure the absorption spectrum around the nuclear resonance with nano-eV resolution.

By contrast, the spectral brilliance of synchrotron-radiation sources exceeds that of radioactive sources by several orders of magnitude. However, the energy spectrum of a synchrotron-radiation source is broad (in contrast to the monoenergetic γ radiation emitted by a radioactive source), and it is delivered in pulses with durations of 50–100 ps (in contrast to the continuously emitting radioactive source). This led to the development of a time-based analogue of Mössbauer spectroscopy: nuclear resonant scattering of synchrotron radiation. This effect was first observed in Bragg scattering geometry (Gerdau *et al.*, 1985) and later in forward scattering geometry (Hastings *et al.*, 1991). Driven by great advances in the development of high-resolution monochromators (Toellner, 2000) and detectors (Baron, 2000), the technique developed rapidly and is now available at all third-generation synchrotron sources worldwide (ESRF, APS, SPring-8 and PETRA III), and is used in a broad range of applications in many fields of the natural sciences. Most of these studies involve the use of the Mössbauer isotope with the highest absorption cross section, which is ^{57}Fe with its 14.4 keV nuclear resonance,

Related chapters

Volume I: 2.1, 2.15, 3.23, 8.7, 8.17

Table 1
List of Mössbauer isotopes that have been used in experiments with synchrotron radiation to date (April 2020).

E is the energy of the resonant transition, a denotes the natural abundance of the isotope, Γ_0 is the natural linewidth of the transition and τ_0 is the corresponding natural lifetime. The reference in the last column points to the first experiment with spectroscopic studies involving the respective isotope.

Isotope	E (keV)	a (%)	Γ_0 (neV)	τ_0 (ns)	Reference
^{181}Ta	6.21	99.9	0.076	8730	Chumakov *et al.* (1995)
^{169}Tm	8.41	100	114	5.8	Sturhahn *et al.* (1991)
^{83}Kr	9.40	12.0	3.13	212	Johnson *et al.* (1995)
^{187}Os	9.78	1.6	217	3.06	Bessas *et al.* (2015)
^{57}Fe	14.41	2.4	4.7	141	Gerdau *et al.* (1985)
^{151}Eu	21.53	47.8	48.4	13.7	Leupold *et al.* (1996)
^{149}Sm	22.49	13.8	64.3	10.3	Röhlsberger *et al.* (2001)
^{119}Sn	23.87	8.6	25.8	25.7	Alp *et al.* (1993)
^{161}Dy	25.61	18.9	15.8	42.0	Shvyd'ko *et al.* (2001)
^{201}Hg	26.27	13.2	762	0.87	Ishikawa *et al.* (2005)
^{40}K	29.83	0.012	111	5.96	Seto *et al.* (2000)
^{125}Te	35.49	7.0	310	2.14	Imai *et al.* (2007)
^{127}I	57.61	100	240	2.76	Yoda *et al.* (2002)
^{121}Sb	37.13	57.25	133	4.99	Wille *et al.* (2006)
^{61}Ni	67.42	1.25	87.2	7.6	Wille *et al.* (2002)
^{73}Ge	68.75	7.76	265	2.5	Simon *et al.* (2013)
^{193}Ir	73.04	62.7	75.4	8.79	Alexeev *et al.* (2019)
^{99}Ru	89.57	12.7	23.0	28.8	Bessas *et al.* (2014)

featuring a recoilless fraction (referred to as the Lamb–Mössbauer factor) of close to 0.8 at room temperature in a metallic environment. There are, however, a number of other Mössbauer isotopes that have been used in experiments with synchrotron radiation and these are listed in Table 1.

Many applications in the field of magnetism use the isotope ^{57}Fe due to its eminent role in magnetic materials, especially in thin films and nanostructures. An example is the magnetic depth profiling of thin films with subnanometre spatial resolution using isotopic probe layers of ^{57}Fe (Röhlsberger *et al.*, 2002). Other isotopes such as ^{119}Sn that do not participate in magnetic interactions can be employed as a probe to monitor the internal magnetic state of a high-T_c superconductor (Troyan *et al.*, 2016), for example. In these applications one analyzes the coherent elastic nuclear resonant scattering from the sample. The temporal beat patterns of the nuclear decay after pulsed excitation are measured, and from these the hyperfine interaction parameters of the nuclei in the sample are derived. In contrast to these coherent elastic methods, the energy dependence of incoherent inelastic scattering opens interesting opportunities to analyze dynamical properties through the application of sum rules.

1.1. Inelastic nuclear resonant scattering

Soon after the discovery of the Mössbauer effect, it became clear that nuclear resonant absorption would be a very sensitive technique to investigate the dynamical properties of nuclei in solids (Singwi & Sjölander, 1960). Resonant nuclei in condensed matter provide a very accurate energy reference with a resolution that is in principle limited only by the natural linewidth of the transition. It turned out, however, that conventional Mössbauer spectroscopy would not be suited to probe atomic dynamics due to the large Doppler velocities required and the reduction of resonant absorption cross sections resulting from the finite lifetimes of vibrational excitations. The situation changed drastically with the advent of high-brilliance synchrotron-radiation sources and tunable X-ray monochromators, providing beams with energy bandwidths in the meV range (Sturhahn *et al.*, 1995). If the energy of such a beam illuminating the sample is off-resonance, nuclear resonance excitation might nevertheless take place if the creation or annihilation of phonons contributes the missing energy. Thus, monitoring the yield $I(E)$ of incoherent delayed nuclear decay products (for example atomic fluorescence photons or conversion electrons) as a function of energy detuning E from the nuclear resonance gives a direct measure of the number of phonon states in the sample, from which quantites such as the phonon density of states (DOS) can be determined. The pulsed time structure of synchrotron radiation permits the use of time-gating techniques to efficiently discriminate the weak delayed nuclear response from the intense nonresonant electronic scattering. Remarkably, $I(E)$ only depends on the phonon population at the very moment when the incident beam hits the sample. For this reason, this technique is able to probe non-equilibrium vibrational states in a pump–probe setup with a time resolution that can be much shorter than the natural lifetime of the nuclei involved (Shenoy & Röhlsberger, 2008).

Quantitatively, in the incoherent scattering process outlined above, the total yield $I(E)$ of delayed fluorescence photons is directly proportional to $S(\mathbf{k}, E)$, a quantity which is the phonon excitation probability function of the sample projected onto the wavevector $\mathbf{k}$ of the incident photons.

Fig. 1 shows a typical phonon spectrum $I(E)$ of α-Fe recorded via inelastic nuclear resonant scattering at the 14.4 keV resonance of ^{57}Fe. With the help of the sum rules discussed below, $I(E)$ can be properly normalized to extract $S(\mathbf{k}, E)$, and higher-order sum rules can be employed to extract thermodynamic properties of the sample.

2. Sum rules

The importance of sum rules is well known in various types of spectroscopy. In optical and electron spectroscopies, for example, they have often been used to derive nontrivial ground-state properties, such as the number of electrons

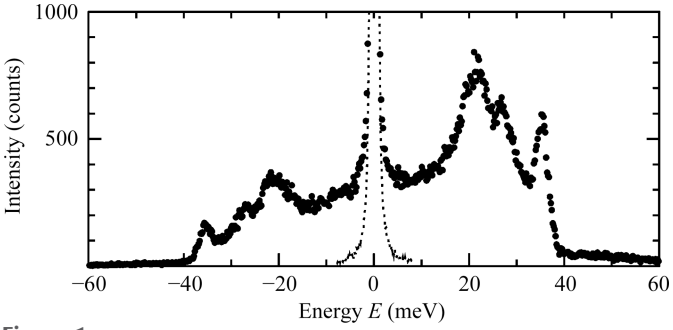

Figure 1
Phonon spectrum of a polycrystalline foil of α-Fe, recorded with an energy resolution of 0.66 meV. The dotted line is the resolution function of the setup. The data are taken from Toellner *et al.* (1997).

participating in a band of optical or electronic transitions, the plasma frequency *etc.* (Smith, 1976; Shiles *et al.*, 1980; Peiponen & Saarinen, 2009; Chantler & Bourke, 2014). In X-ray absorption spectroscopy with circularly polarized synchrotron radiation, sum rules were developed to determine the orbital and spin moments of the atomic species in the sample (Thole *et al.*, 1992; Carra *et al.*, 1993; Altarelli, 1993; Chen *et al.*, 1995).

A special class of spectroscopic sum rules are applied to the various moments of the measured spectra. These so-called moment sum rules have been developed in many areas of physics where a sudden momentum transfer occurs on an effectively point-like constituent of a bound system, including X-ray and neutron scattering (Ott, 1935; Lamb, 1939; Van Hove, 1954; Singwi & Sjölander, 1960) as well as lepton pair emission by heavy quarks bound in hadrons (Lipkin, 1993). The general formulation of these sum rules is essentially the same for all processes, but the applications to data analyses for individual processes can be very different (Lipkin, 1995).

Nuclear resonant scattering of photons from a synchrotron source fulfils the condition of sudden momentum transfer because the resonant interaction of a Mössbauer nucleus with a photon is a two-step process with prompt absorption and delayed re-emission. This process can either proceed with recoil, *i.e.* involve the creation or annihilation of a phonon upon the absorption of the photon, or may frequently include recoil-free transitions that lead to coherent forward scattering from different nuclei. These features, which are completely absent, for example, in neutron scattering, play a crucial role in data analysis of inelastic nuclear resonant scattering. Moment sum rules are extremely valuable to derive elastic and thermodynamic properties of the sample from the measured vibrational spectra (Lipkin, 1995; Hu *et al.*, 2013), as will be shown in the following.

2.1. Moments of $S(E)$

Moment sum rules of the Mössbauer energy spectrum were studied soon after the discovery of the Mössbauer effect to help to understand the effect and reveal its quantum nature (Lipkin, 1962). First and second moments were studied in detail, and the general formulae were set out. After the initial discovery of nuclear resonance inelastic X-ray scattering (NRIXS; Sturhahn *et al.*, 1995; Seto *et al.*, 1995), the sum rules were extended up to the fourth moment in the context of harmonic approximation (Lipkin, 1995). In particular, the third moment of a measured spectrum was shown to be related to a mean force constant. Since then, the results have also been presented in many different contexts (Kohn *et al.*, 1998, 2006; Lipkin, 1999; Chumakov & Sturhahn, 1999; Kohn & Chumakov, 2000; Sturhahn, 2004; Hu *et al.*, 2013).

Our focus is on the physical interpretation of the moments; that is, the relations of these moments to atomic dynamical properties. It turns out that the central moments of $S(\mathbf{k}, E)$ with respect to the nuclear recoil energy E_R have more straightforward interpretations.

$$R_l(\mathbf{k}) \equiv \int (E - E_\mathrm{R})^l S(\mathbf{k}, E)\, \mathrm{d}E. \tag{1}$$

It has been established that the first few low-order moments are

$$R_0 = 1, \tag{2}$$

$$R_1 = 0, \tag{3}$$

$$R_2 = 4E_\mathrm{R} T_{\hat{\mathbf{k}}}, \tag{4}$$

$$R_3 = \frac{\hbar^2 E_\mathrm{R}}{\tilde{m}} \left\langle \frac{\partial^2 V}{\partial z^2} \right\rangle. \tag{5}$$

Here $\tilde{m}$ is the mass of a resonance nucleus, $\hat{\mathbf{k}} = \mathbf{k}/k$ is the unit vector along the incident photon direction and z is the coordinate along this direction. Their derivations can be found elsewhere (Hu *et al.*, 2013). The first equation expresses the normalization of $S(\mathbf{k}, E)$. The vanishing first moment provides a means to normalize the measured spectrum to obtain $S(\mathbf{k}, E)$, because the elastic peak in a measured spectrum has a different normalization to the rest of the spectrum (Lipkin, 1995; Sturhahn *et al.*, 1995; Hu *et al.*, 2013).

One very important feature of NRIXS is its directional dependence (Chumakov *et al.*, 1997). The energy of nuclear resonant absorption is modified through atomic thermal motions; specifically, the atomic motions along the incident photon direction. To emphasize this characteristic and be concise, we shall use 'projected' as a qualifier to describe many of the quantities derived from an NRIXS measurement, as in the often-used term projected phonon DOS.

The second moment is related to the mean kinetic energy from atomic motion along $\hat{\mathbf{k}}$. For an isotropic sample it is 1/3 of the mean kinetic energy per nucleus and, by the virial theorem, 1/6 of the internal energy per atom.

For the third moment, the angle brackets represent thermodynamic and quantum-mechanical expectation values, where the lattice Hamiltonian is

$$H = \sum_{\mu}^{N} \frac{\mathbf{p}_\mu^2}{2m_\mu} + V(\mathbf{r}_1, \mathbf{r}_2, \ldots, \mathbf{r}_N) \tag{6}$$

and V is the many-body lattice potential. Beyond the harmonic model, considering an anharmonic potential up to the quartic term, we have

$$\frac{\partial^2 V}{\partial z^2} = K_{\hat{\mathbf{k}}} + A_{\hat{\mathbf{k}}} z + \frac{B_{\hat{\mathbf{k}}}}{2} z^2, \tag{7}$$

with coefficients that are evaluated at the equilibrium atomic positions. They are, respectively, the directional force constant (the only term left in a quasi-harmonic approximation) and the third-order and fourth-order coupling parameters along the $\hat{\mathbf{k}}$ direction. For a sample at equilibrium, the mean displacement in any direction is zero; thus, we can neglect the A term to yield

$$R_3 = \frac{\hbar^2 E_\mathrm{R}}{\tilde{m}} \left(K_{\hat{\mathbf{k}}} + \frac{B_{\hat{\mathbf{k}}}}{2} \langle z^2 \rangle \right), \tag{8}$$

where $\langle z^2 \rangle$ is the atomic mean-square displacement in the $\hat{\mathbf{k}}$ direction, which can be calculated from the directional Lamb–Mössbauer factor or f-factor, which can be determined from a

measured NRIXS spectrum (Hu *et al.*, 2013). The mean-square displacement varies with either temperature or pressure, or both. If one plots R_3 versus $\langle z^2 \rangle$, the slope at each point is the coefficient $B_{\hat{\mathbf{k}}}$ of the quartic term in the lattice potential and the y intercept is the mean force constant under the corresponding condition. This indicates a way of directly measuring the anharmonic corrections to a lattice potential.

The fourth moment involves the mean-square force and mean quartic momentum along $\hat{\mathbf{k}}$, as well as mixed terms (Hu *et al.*, 2013).

The moments as expressed in these sum rules can be calculated, given any specific model of lattice potentials, and the results can be compared with the moments of a measured spectrum. This may be used to restrict and adjust models of lattice potentials.

2.2. DOS moments and lattice thermodynamics

While moments of $S(\mathbf{k}, E)$ give some averaged properties of atomic dynamics, the spectrum itself contains much more detailed information. A critical step in the development of NRIXS was the realization that phonon DOS could be derived from an NRIXS spectrum (Sturhahn *et al.*, 1995), which is performed in the context of the quasi-harmonic lattice model. The derivation has been described many times before (Sturhahn & Kohn, 1999; Hu, 1999; Röhlsberger, 2001; Sturhahn, 2004).

Projected partial phonon DOS (ppDOS) characterizes the vibrational dynamics of a resonant nuclei sublattice. Its detailed structure is related to the relevant vibrational modes, while the moments and weighted integrals provide atomic dynamics as well as macroscopic thermodynamic properties. Again, we should emphasize that these quantities are contributions from the atomic motions along incident photon direction $\hat{\mathbf{k}}$.

Let us define the regular moments of ppDOS,

$$g_l(\mathbf{k}) \equiv \int E^l \mathcal{D}(\mathbf{k}, E)\, \mathrm{d}E, \tag{9}$$

and the thermally averaged moments,

$$\tilde{g}_l(\mathbf{k}) \equiv \int \left[n(E) + \tfrac{1}{2}\right] E^l \mathcal{D}(\mathbf{k}, E)\, \mathrm{d}E, \tag{10}$$

where $n(E)$ are phonon occupation numbers. These are useful quantities since they carry information on thermal excitation, which allows the temperature effect to be studied. Both definitions can be expressed in a unified fashion, as shown in Kohn & Chumakov (2000), where $\tilde{g}_{-1}$ to $\tilde{g}_2$ were expressed.

Various dynamics and thermodynamic quantities can be calculated from ppDOS derived from an NRIXS measurement (Alp *et al.*, 2002; Hu *et al.*, 2013), including the mean-square displacement along the photon direction, the projected partial mean kinetic energy, the internal energy, the Helmholtz free energy, the vibrational entropy and the isochoric specific heat, as well as several types of force constants.

2.3. Moment relations

In the previous sections we have described both the NRIXS spectrum $S(\mathbf{k}, E)$ and the projected partial phonon DOS $\mathcal{D}(\mathbf{k}, E)$, and their own sets of moments. Mathematically these two functions are equivalent in a quasi-harmonic lattice model, in the sense that at any given temperature one can be derived from the other. As a result, relationships exist between the two sets of moments (Hu *et al.*, 2013).

This reveals that in a quasi-harmonic model, even though $S(\mathbf{k}, E)$ is a function of temperature, its first and third moments are not. One of the relations provides an interpretation of the mean force constant $K_{\hat{\mathbf{k}}}$ along the photon direction as a weighted average of all force constants of each normal mode.

These relations can be employed to check the consistency of the derived phonon DOS with an NRIXS spectrum. One can also estimate thermodynamic properties from an NRIXS measurement. Many thermodynamic functions or their approximations are expressed in DOS moments. Thus, one can make estimations based on the moments of an NRIXS spectrum. A study of iron-isotope fractionation used this approach to calculate β-factors, the reduced partition function ratios, from NRIXS measurements (Dauphas *et al.*, 2012).

References

Alexeev, P., Leupold, O., Sergueev, I., Herlitschke, M., McMorrow, D. F., Perry, R. S., Hunter, E., Röhlsberger, R. & Wille, H.-C. (2019). *Sci. Rep.* **9**, 5097.

Alp, E. E., Mooney, T. M., Toellner, T., Sturhahn, W., Witthoff, E., Röhlsberger, R., Gerdau, E., Homma, H. & Kentjana, M. (1993). *Phys. Rev. Lett.* **70**, 3351–3354.

Alp, E. E., Sturhahn, W., Toellner, T. S., Zhao, J., Hu, M. & Brown, D. E. (2002). *Hyperfine Interact.* **144/145**, 3–20.

Altarelli, M. (1993). *Phys. Rev. B*, **47**, 597–598.

Baron, A. Q. R. (2000). *Hyperfine Interact.* **125**, 29–42.

Bessas, D., Merkel, D. G., Chumakov, A. I., Rüffer, R., Hermann, R. P., Sergueev, I., Mahmoud, A., Klobes, B., McGuire, M. A., Sougrati, M. T. & Stievano, L. (2014). *Phys. Rev. Lett.* **113**, 147601.

Bessas, D., Sergueev, I., Merkel, D. G., Chumakov, A. I., Rüffer, R., Jafari, A., Kishimoto, S., Wolny, J. A., Schünemann, V., Needham, R. J., Sadler, P. J. & Hermann, R. P. (2015). *Phys. Rev. B*, **91**, 224102.

Carra, P., Thole, B. T., Altarelli, M. & Wang, X. (1993). *Phys. Rev. Lett.* **70**, 694–697.

Chantler, C. T. & Bourke, J. D. (2014). *Phys. Rev. B*, **90**, 174306.

Chen, C. T., Idzerda, Y. U., Lin, H., Smith, N. V., Meigs, G., Chaban, E., Ho, G. H., Pellegrin, E. & Sette, F. (1995). *Phys. Rev. Lett.* **75**, 152–155.

Chumakov, A. I., Baron, A. Q. R., Arthur, J., Ruby, S. L., Brown, G. S., Smirnov, G. V., van Bürck, U. & Wortmann, G. (1995). *Phys. Rev. Lett.* **75**, 549–552.

Chumakov, A. I., Rüffer, R., Baron, A. Q. R., Grünsteudel, H., Grünsteudel, H. F. & Kohn, V. G. (1997). *Phys. Rev. B*, **56**, 10758–10761.

Chumakov, A. I. & Sturhahn, W. (1999). *Hyperfine Interact.* **123/124**, 781–808.

Dauphas, N., Roskosz, M., Alp, E. E., Golden, D. C., Sio, C. K., Tissot, F. L. H., Hu, M. Y., Zhao, J., Gao, L. & Morris, R. V. (2012). *Geochim. Cosmochim. Acta*, **94**, 254–275.

Gerdau, E., Rüffer, R., Winkler, H., Tolksdorf, W., Klages, C. P. & Hannon, J. P. (1985). *Phys. Rev. Lett.* **54**, 835–838.

Hastings, J. B., Siddons, D. P., van Bürck, U., Hollatz, R. & Bergmann, U. (1991). *Phys. Rev. Lett.* **66**, 770–773.

Hu, M. Y. (1999). PhD Dissertation. Northwestern University, Evanston, Illinois, USA.

Hu, M. Y., Toellner, T. S., Dauphas, N., Alp, E. E. & Zhao, J. (2013). *Phys. Rev. B*, **87**, 064301.

Imai, Y., Yoda, Y., Kitao, S., Masuda, R., Higashitaniguchi, S., Inaba, C. & Seto, M. (2007). *Proc. SPIE*, **6705**, 670512.
Ishikawa, I., Baron, A. Q. R. & Ishikawa, T. (2005). *Phys. Rev. B*, **72**, 140301.
Johnson, D. E., Siddons, D. P., Larese, J. Z. & Hastings, J. B. (1995). *Phys. Rev. B*, **51**, 7909–7911.
Kohn, V. G. & Chumakov, A. I. (2000). *Hyperfine Interact.* **125**, 205–221.
Kohn, V. G., Chumakov, A. I. & Rüffer, R. (1998). *Phys. Rev. B*, **58**, 8437–8444.
Kohn, V. G., Chumakov, A. I. & Rüffer, R. (2006). *Phys. Rev. B*, **73**, 094306.
Lamb, W. E. (1939). *Phys. Rev.* **55**, 190–197.
Leupold, O., Pollmann, J., Gerdau, E., Rüter, H. D., Faigel, G., Tegze, M., Bortel, G., Rüffer, R., Chumakov, A. I. & Baron, A. Q. R. (1996). *Europhys. Lett.* **35**, 671–676.
Lipkin, H. J. (1962). *Ann. Phys.* **18**, 182–197.
Lipkin, H. J. (1993). *Nucl. Phys. A*, **560**, 548–558.
Lipkin, H. J. (1995). *Phys. Rev. B*, **52**, 10073–10079.
Lipkin, H. J. (1999). *Hyperfine Interact.* **123/124**, 349–366.
Ott, H. (1935). *Ann. Phys.* **415**, 169–196.
Peiponen, K.-E. & Saarinen, J. J. (2009). *Rep. Prog. Phys.* **72**, 056401.
Röhlsberger, R. (2001). *J. Phys. Condens. Matter*, **13**, 7659–7677.
Röhlsberger, R., Quast, K. W., Toellner, T. S., Lee, P. L., Sturhahn, W., Alp, E. E. & Burkel, E. (2001). *Phys. Rev. Lett.* **87**, 047601.
Röhlsberger, R., Thomas, H., Schlage, K., Burkel, E., Leupold, O. & Rüffer, R. (2002). *Phys. Rev. Lett.* **89**, 237201.
Seto, M., Kitao, S., Kobayashi, Y., Haruki, R., Mitsui, T., Yoda, Y., Zhang, X. W. & Maeda, Y. (2000). *Phys. Rev. Lett.* **84**, 566–569.
Seto, M., Yoda, Y., Kikuta, S., Zhang, X. W. & Ando, M. (1995). *Phys. Rev. Lett.* **74**, 3828–3831.
Shenoy, G. K. & Röhlsberger, R. (2008). *Hyperfine Interact.* **182**, 157–172.
Shiles, E., Sasaki, T., Inokuti, M. & Smith, D. Y. (1980). *Phys. Rev. B*, **22**, 1612–1628.
Shvyd'ko, Y. V., Gerken, M., Franz, H., Lucht, M. & Gerdau, E. (2001). *Europhys. Lett.* **56**, 309–315.
Simon, R., Sergueev, I., Persson, J., McCammon, C. A., Hatert, F. & Hermann, R. P. (2013). *Europhys. Lett.* **104**, 17006.
Singwi, K. S. & Sjölander, A. (1960). *Phys. Rev.* **120**, 1093–1102.
Smith, D. Y. (1976). *Phys. Rev. B*, **13**, 5303–5315.
Sturhahn, W. (2004). *J. Phys. Condens. Matter*, **16**, S497–S530.
Sturhahn, W., Gerdau, E., Hollatz, R., Rüffer, R., Rüter, H. D. & Tolksdorf, W. (1991). *Europhys. Lett.* **14**, 821–825.
Sturhahn, W. & Kohn, V. (1999). *Hyperfine Interact.* **123/124**, 367–399.
Sturhahn, W., Toellner, T. S., Alp, E. E., Zhang, X., Ando, M., Yoda, Y., Kikuta, S., Seto, M., Kimball, C. W. & Dabrowski, B. (1995). *Phys. Rev. Lett.* **74**, 3832–3835.
Thole, B. T., Carra, P., Sette, F. & van der Laan, G. (1992). *Phys. Rev. Lett.* **68**, 1943–1946.
Toellner, T. S. (2000). *Hyperfine Interact.* **125**, 3–28.
Toellner, T. S., Hu, M. Y., Sturhahn, W., Quast, K. W. & Alp, E. E. (1997). *Appl. Phys. Lett.* **71**, 2112–2114.
Troyan, I., Gavriliuk, A., Rüffer, R., Chumakov, A. I., Mironovich, A., Lyubutin, I., Perekalin, D., Drozdov, A. P. & Eremets, M. I. (2016). *Science*, **351**, 1303–1306.
Van Hove, L. (1954). *Phys. Rev.* **95**, 249–262.
Wille, H.-C., Gerken, M., Gerdau, E., Shvyd'ko, Y. V., Rüter, H. D. & Franz, H. (2002). *Hyperfine Interactions (C)*, edited by M. F. Thomas, J. M. Williams & T. C. Gibb, pp. 1–4. Dordrecht: Springer.
Wille, H.-C., Shvyd'ko, Y. V., Alp, E. E., Rüter, D., Leupold, O., Sergueev, I., Rüffer, R., Barla, A. & Sanchez, J. P. (2006). *Europhys. Lett.* **74**, 170–176.
Yoda, Y., Kishimoto, S., Zhang, X. W., Seto, M. & Kikuta, S. (2002). *Hyperfine Interactions (C)*, edited by M. F. Thomas, J. M. Williams & T. C. Gibb, pp. 17–20. Dordrecht: Springer.